Bulletin of the Seismological Society of America, Vol. 99, No. 2B, pp. 1416–1422, May 2009, doi: 10.1785/0120080152

Short Note

Waves in Linear Elastic Media with Microrotations, Part 1: Isotropic Full Cosserat Model

by Mikhail Kulesh

Abstract In this article, we consider a problem of the surface elastic wave propagation within the framework of the isotropic Cosserat continuum. The medium deformation in this model is described not only by the displacement vector but also by a kinematically independent rotation vector. We discuss the general solution of equations of motion. This solution describes the following wave types: longitudinal and transverse bulk waves, Rayleigh wave, surface transverse wave in a half-space as well as Lamb wave and transverse wave in a thin layer. Within the framework of Cosserat continuum, both the Rayleigh and surface transverse waves in a half-space are dispersive. The transverse wave in a thin layer and the surface transverse wave in a half-space do not have any analogies in the classical elasticity theory.

Introduction

The interpretation of seismic data is usually based on a physical model of a continuous medium. Probably the most popular and well-investigated model is the theory of classical elasticity. Its applications to seismology are described in detail by Aki and Richards (2002). In this model, the motion of medium particles is fully determined by the vector of translational displacement, and the wave propagation is described by the Lamé linear differential equations. Generalizations of this model for plastic, viscoelastic, thermoelastic, and heterogeneous media are also widely used. However, as with the classical elasticity theory, the particle motion in all these models is described by the displacement vector $\mathbf{u}$ only.

However, there are works based on experimental data (e.g., Twiss *et al.*, 1993) that underline the importance of the rotational degrees of freedom in seismology. The question if rotations are necessary in seismology for the description of the medium behavior can be answered by a correctly performed experiment using modern experimental equipment. Currently, there are mechanical (Nigbor, 1994) and laser (Igel *et al.*, 2005) sensors that allow direct measurements of rotation velocities in three orthogonal directions. This equipment is currently (though not widely) used in seismic and geophysical studies. Therefore, the question arises, how can these rotations be described in the framework of an elastic medium?

In the deformation process, generally speaking, the macrorotations corresponding to the vortex deformation $1/2\,\mathrm{rot}\,\mathbf{u}$ are always present. However, the proper rotational dynamics of medium particles, microspin, can also exist. For the first time the theory of a continuum with rotational interaction of particles was suggested by Cosserat and Cosserat (1909). In this theory, the stress tensor is asymmetric, and a couple-stress tensor describing torque interaction is introduced. The deformation of the medium is described not only by the symmetric Cauchy–Green strain tensor but also by other asymmetric tensors depending on an angular and a mixed type of strain. In the second half of the twentieth century, this theory was developed in various works. This class of theories is called Cosserat-type models or asymmetric elasticity theories.

In many papers (see, for example, Savin *et al.*, 1970), it is assumed that the components of the rotation and displacement vectors are linked by a relation that corresponds to the classical theory of elasticity or the Cosserat pseudocontinuum theory, $\boldsymbol{\theta} = 1/2\,\mathrm{rot}\mathbf{u}$, but the stress tensor is still asymmetric.

In the full linear Cosserat theory described by Nowacki (1975) and Eringen (1998), the rotation vector $\boldsymbol{\theta}$ and the displacement vector $\mathbf{u}$ are kinematically independent. On the one hand, this leads to an increase in the number of necessary material parameters. On the other, from a physical point of view, the full theory is more realistic than the Cosserat pseudocontinuum theory. However, there are still no experimental data on the nature of the relationship between the displacement and rotation vectors.

Wave experiments, especially in geological media, provide information for the identification of models of asymmetric media. Such experiments have been performed; in particular, results of ultrasonic studies of homogeneous media were used to identify the Le Roux model and the Cosserat pseudocontinuum model by Erofeev (1999) and to identify the linear Cosserat continuum model by Gauthier

and Jahsman (1981) and Lakes (1995). Geological media are more complex subjects of research because several types of waves are simultaneously excited and recorded in them, longitudinal and transverse direct and reflected bulk waves, Rayleigh waves, Love waves, Lamb, and Stonely waves.

In this part of the article, we discuss the generalization of some solutions for plane waves in a Cosserat continuum. We consider longitudinal and transverse bulk waves of displacement and rotation (Kulesh *et al.*, 2008), Rayleigh wave (Kulesh *et al.*, 2005), surface transverse wave in the half-space (Kulesh *et al.*, 2006), and the Lamb wave as well as the transverse wave in a thin layer (Kulesh *et al.*, 2007). The transverse wave in a thin layer and surface transverse wave in the half-space do not have any analogies in the classical elasticity theory. This article summarizes the results obtained in the four works cited previously. First, we present basic solutions in a different form from those discussed by Eringen (1998) and Nowacki (1975) because our form is more convenient for the application purposes. Second, we give the graphical illustration and physical interpretation, which allows us to understand the character of the solutions, its similarities, differences from the classical theory, and typical features of the medium behavior.

The Basic Equations for the Cosserat Medium

Each material point in the asymmetric theory of elasticity within the framework of the Cosserat medium is an infinitesimal solid that has an orientation. The solid load is transmitted by distributed force $\mathbf{p} = \mathbf{n} \cdot \tilde{\sigma}$ and distributed moment of force $\mathbf{m} = \mathbf{n} \cdot \tilde{\mu}$, which have an effect on a surface with a normal vector $\mathbf{u}$. In this case, a particle's kinematics are described by the displacement vector $\mathbf{u} = \{u_x, u_y, u_z\}$ of the center of mass and by the rotation vector $\boldsymbol{\theta} = \{\theta_x, \theta_y, \theta_z\}$. In the case of the Cosserat medium, both vectors are continuous functions of spatial coordinates and time. Thus, we describe the elastic Cosserat continuum by the following tensors and equations (Nowacki, 1975):

- Asymmetric strain tensor $\tilde{\gamma} = \nabla \boldsymbol{u} - \tilde{\mathbf{E}} \cdot \boldsymbol{\theta}$ and asymmetric torsion bending tensor $\tilde{\chi} = \nabla \boldsymbol{\theta}$,
- Asymmetric stress tensor $\tilde{\sigma} = 2\mu\tilde{\gamma}^{(S)} + 2\alpha\tilde{\gamma}^{(A)} + \lambda I_1(\tilde{\gamma})\tilde{e}$ and asymmetric couple-stress tensor $\tilde{\mu} = 2\gamma\tilde{\chi}^{(S)} + 2\varepsilon\tilde{\chi}^{(A)} + \beta I_1(\tilde{\chi})\tilde{e}$, and
- Equations of motion for the case of spherical inertia tensor $j\tilde{e}$ (j is the inertia moment density, $\tilde{e}$ is the unit tensor) and zero mass forces and torques

$$\begin{aligned}(2\mu + \lambda)\text{grad div}\mathbf{u} - (\mu + \alpha)\text{rot rot}\mathbf{u} + 2\alpha\,\text{rot}\boldsymbol{\theta} = \rho\ddot{\mathbf{u}},\\ (\beta + 2\gamma)\text{grad div}\boldsymbol{\theta} - (\gamma + \varepsilon)\text{rot rot}\boldsymbol{\theta} + 2\alpha\,\text{rot}\mathbf{u}\\ -4\alpha\boldsymbol{\theta} = j\ddot{\boldsymbol{\theta}}.\end{aligned} \tag{1}$$

In equations (1), μ and λ are the Lamé constants; α, β, γ, and ε are the physical constants of a material in the framework of the Cosserat medium; ρ is the density; $(.)^{(S)}$ and $(.)^{(A)}$ denote the symmetric and antisymmetric parts of tensor; $\tilde{\mathbf{E}}$ is the Levi–Civita tensor of the third rank; and $I_1(.)$ is the first invariant of the tensor. It is important to note that, unlike the classical theory of elasticity, the displacement vector $\mathbf{u}$ and the rotation vector $\boldsymbol{\theta}$ are independent.

Construction of the General Solution of a Plane Wave

Let us consider a half-space or a thin layer whose surfaces are free from load when there are no mass forces and moments. We choose the x and y Cartesian axes along the surface and the z axis upward. Let the wave propagate in the positive x direction.

Unlike previous works (Lyalin *et al.*, 1982; Eringen, 1998) where only monochromatic waves are considered, here we represent the general solution of equation (1) in the form of Fourier integrals of all components of the displacement and rotation vectors, which means that the solution is represented as a plane wave packet limited in the time and Fourier domains:

$$\begin{aligned}u_r(x, z, t, k) &= \int_{-\infty}^{\infty} U_r(z) e^{i(kx+\omega t)} \hat{s}_0(\omega)\ d\omega,\\ \theta_r(x, z, t, k) &= \int_{-\infty}^{\infty} W_r(z) e^{i(kx+\omega t)} \hat{s}_0(\omega)\ d\omega,\end{aligned} \tag{2}$$

where i is the imaginary unit, k is the wavenumber, ω is the circular frequency, t is the time, $U_r(z)$ and $W_r(z)$ are amplitude functions depending on depth only, and $\hat{s}_0(\omega)$ is the complex spectral function corresponding to the Fourier spectrum of a source signal that determines the wave packet form. The subscript r takes values x, y, and z.

It is expedient to use the continuous Fourier transform of equations (1) and (2):

$$\begin{aligned}&(2\mu + \lambda)\text{grad div}\hat{\mathbf{u}} - (\mu + \alpha)\text{rot rot}\hat{\mathbf{u}} + 2\alpha\,\text{rot}\hat{\boldsymbol{\theta}}\\ &\qquad + \rho\omega^2\hat{\mathbf{u}} = 0,\\ &(\beta + 2\gamma)\text{grad div}\hat{\boldsymbol{\theta}} - (\gamma + \varepsilon)\text{rot rot}\hat{\boldsymbol{\theta}} + 2\alpha\,\text{rot}\hat{\mathbf{u}}\\ &\quad -(4\alpha - j\omega^2)\hat{\boldsymbol{\theta}} = 0,\\ &\qquad \hat{\mathbf{u}} = \{U_x(z), U_y(z), U_z(z)\}^T e^{ikx}\hat{s}_0(\omega),\\ &\qquad \hat{\boldsymbol{\theta}} = \{W_x(z), W_y(z), W_z(z)\}^T e^{ikx}\hat{s}_0(\omega).\end{aligned} \tag{3}$$

For the convenience of representation, we reduce all the quantities to the dimensionless form using the characteristic length X_0 and the characteristic frequency ω_0 and introduce some dimensionless variables, one of which depends on the characteristic length:

$$A = X_0\sqrt{\frac{\mu}{B(\gamma + \varepsilon)}}, \qquad B = \frac{\alpha + \mu}{\alpha},$$
$$C = \frac{\gamma - \varepsilon}{\gamma + \varepsilon}, \qquad F = \frac{B - 1}{A^2 B}.$$

Dynamic effects are taken into account by using the dimensionless velocities:

$$C_1^2 = \frac{\lambda + 2\mu}{\rho X_0^2 \omega_0^2}, \qquad C_2^2 = \frac{\mu}{\rho X_0^2 \omega_0^2}, \qquad C_3^2 = \frac{B}{B-1} C_2^2,$$
$$C_4^2 = \frac{\gamma + \varepsilon}{j X_0^2 \omega_0^2}, \qquad C_5^2 = \frac{\beta + 2\gamma}{j X_0^2 \omega_0^2}. \tag{4}$$

To obtain the solution of equations of motion, we use the method that is exhaustively described by Kulesh *et al.* (2005, 2006) as applied to equations (3). If we substitute the variables $\mathbf{u}$ and $\hat{\boldsymbol{\theta}}$ into equation (3), we obtain a system of differential equations for functions $U_r(z)$ and $W_r(z)$. When we solve these equations, we keep not only the terms showing depth dependent decay but also all partial solutions. After we found functions $U_r(z)$ and $W_r(z)$ and pass on to the time domain using representation (2), we can write the general solution of equation (1) in the following form:

It is important to note that these exponents depend on two free variables, wavenumber k and circular frequency ω. The relationship between these two variables will be defined later by analyzing dispersion equations of particular wave types.

Below, we will give dependences of the wavenumber on frequency as well as plot corresponding dispersion curves for the following values of material parameters, $\lambda = 2.8 \cdot 10^{10}$ N/m^2, $\mu = 4 \cdot 10^9$ N/m^2, $\rho = 10^5$ kg/m^3, $\alpha = 2 \cdot 10^9$ N/m^2, $\beta = 10^8$ N, $\gamma = 1.936 \cdot 10^8$ N, $\varepsilon = 3.0464 \cdot 10^9$ N, and $j = 10^4$ kg/m.

Analytical Solutions for Body Waves

Solutions for bulk longitudinal waves are obtained directly from equation (3) using the conditions that amplitude functions are independent from vertical coordinate z: $U_x(z) = U_x$, $U_y(z) = 0$, $U_z(z) = 0$, $W_x(z) = W_x$, $W_y(z) = 0$, and $W_z(z) = 0$, where $z \in \mathbb{R}$. After substituting these con-

$$\begin{aligned}
u_x(x,z,t) &= \int_{-\infty}^{\infty} \{D_1 ike^{-\nu_1 z} + D_2 \nu_2 e^{-\nu_2 z} + D_3 \nu_3 e^{-\nu_3 z} + D_4 ike^{\nu_1 z} - D_5 \nu_2 e^{\nu_2 z} - D_6 \nu_3 e^{\nu_3 z}\} e^{i(kx+\omega t)} \hat{s}_0(\omega) d\omega, \\
u_y(x,z,t) &= \frac{F}{2} \int_{-\infty}^{\infty} \left\{ E_2 \left(A_m - \frac{\omega^2}{C_4^2} + \frac{4}{F} \right) e^{-\xi_2 z} + E_3 \left(A_p - \frac{\omega^2}{C_4^2} + \frac{4}{F} \right) e^{-\xi_3 z} + E_5 \left(A_m - \frac{\omega^2}{C_4^2} + \frac{4}{F} \right) e^{\xi_2 z} \right. \\
&\quad \left. + E_6 \left(A_p - \frac{\omega^2}{C_4^2} + \frac{4}{F} \right) e^{\xi_3 z} \right\} e^{i(kx+\omega t)} \hat{s}_0(\omega) d\omega, \\
u_z(x,z,t) &= \int_{-\infty}^{\infty} \{-D_1 \nu_1 e^{-\nu_1 z} + D_2 ike^{-\nu_2 z} + D_3 ike^{-\nu_3 z} + D_4 \nu_1 e^{\nu_1 z} + D_5 ike^{\nu_2 z} + D_6 ike^{\nu_3 z}\} e^{i(kx+\omega t)} \hat{s}_0(\omega) d\omega, \\
\theta_x(x,z,t) &= \int_{-\infty}^{\infty} \{E_1 ike^{-\xi_1 z} + E_2 \xi_2 e^{-\xi_2 z} + E_3 \xi_3 e^{-\xi_3 z} + E_4 ike^{\xi_1 z} - E_5 \xi_2 e^{\xi_2 z} - E_6 \xi_3 e^{\xi_3 z}\} e^{i(kx+\omega t)} \hat{s}_0(\omega) d\omega, \\
\theta_y(x,z,t) &= \frac{B}{2} \int_{-\infty}^{\infty} \left\{ D_2 \left(A_m - \frac{\omega^2}{C_3^2} \right) e^{-\nu_2 z} + D_3 \left(A_p - \frac{\omega^2}{C_3^2} \right) e^{-\nu_3 z} + D_5 \left(A_m - \frac{\omega^2}{C_3^2} \right) e^{\nu_2 z} \right. \\
&\quad \left. + D_6 \left(A_p - \frac{\omega^2}{C_3^2} \right) e^{\nu_3 z} \right\} e^{i(kx+\omega t)} \hat{s}_0(\omega) d\omega, \\
\theta_z(x,z,t) &= \int_{-\infty}^{\infty} \{-E_1 \xi_1 e^{-\xi_1 z} + E_2 ike^{-\xi_2 z} + E_3 ike^{-\xi_3 z} + E_4 \xi_1 e^{\xi_1 z} + E_5 ike^{\xi_2 z} + E_6 ike^{\xi_3 z}\} e^{i(kx+\omega t)} \hat{s}_0(\omega) d\omega.
\end{aligned} \tag{5}$$

The constants D_s and E_s ($s = 1 \ldots 6$) must be determined from the boundary conditions, while the exponents of the amplitude functions, ν_r and ξ_r, ($r = 1 \ldots 3$) are given by the expressions:

$$\nu_1 = \sqrt{k^2 - \frac{\omega^2}{C_1^2}}, \qquad \xi_1 = \sqrt{k^2 - \frac{\omega^2}{C_5^2} + \frac{4C_4^2}{FC_5^2}}, \qquad \nu_2 = \xi_2 = \sqrt{k^2 - A_m}, \qquad \nu_3 = \xi_3 = \sqrt{k^2 - A_p},$$
$$A_{p,m} = \frac{C_3^2 + C_4^2}{2C_3^2 C_4^2} \omega^2 - 2A^2 \pm \sqrt{\frac{(C_3^2 - C_4^2)^2}{4C_3^4 C_4^4} \omega^4 - \frac{2A^2 (C_2^2 C_3^2 - 2C_3^2 C_4^2 + C_2^2 C_4^2)}{C_2^2 C_3^2 C_4^2} \omega^2 + 4A^4}.$$

ditions in equation (3), two independent dispersion equations are derived, one of which corresponds to the longitudinal wave of displacements and the other to the longitudinal wave of rotations:

$$(\rho\omega^2 - k^2(\lambda + 2\mu))U_x = 0,$$
$$(j\omega^2 - k^2(\beta + 2\gamma) - 4\alpha)W_x = 0.$$

Using dimensionless parameters C_1 and C_5 as given in equation (4), we can rewrite and solve these equations in a dimensionless form that gives us two dispersion curves:

$$k_1(\omega) = \frac{\omega}{C_1}, \qquad k_2(\omega) = \sqrt{\frac{\omega^2}{C_5^2} - k_0^2}, \qquad k_0 = 2X_0\sqrt{\frac{\alpha}{\beta + 2\gamma}}. \tag{6}$$

To plot these curves, we pass on to dimension form, using $X_0 = 1$ and $\omega_0 = 1$. Figure 1a shows the phase velocities $C_{p,1} = \omega/k_1(\omega)$ and $C_{p,2} = \omega/k_2(\omega)$. The solid line depicts well-known dispersion curve $C_{p,1}$ of the longitudinal wave of displacements. At the same time, an independent and dispersed wave of rotations appears in the medium (dashed line) that has the phase velocity $C_{p,2}$ and the lower frequency $w_0 = 2\sqrt{\alpha/j}$ (vertical dotted line). As seen, the velocity C_5 (horizontal dotted line) is limiting for the velocity curve of this rotation wave. Thus, in addition to the longitudinal wave velocity C_1, we should introduce the parameter C_5 associated with the velocity of the longitudinal wave of rotations. Besides, the latter wave has a forbidden frequency domain characterized by the quantity k_0, which is the limit wavenumber.

A solution for the transverse plane wave can be obtained similarly:

$$k_3(\omega) = \sqrt{A_p}, \qquad k_4(\omega) = \sqrt{A_m}. \tag{7}$$

Equation (7) has the following interpretation. First, the transverse wave in the Cosserat continuum has two wave modes with the wavenumbers $k_3(\omega)$ and $k_4(\omega)$. (For an isotropic medium, the horizontally and vertically polarized transverse waves are indistinguishable; therefore, each of them has two wave modes.) This distinguishes equation (7) from the classical case in which there is only one wave mode. Second, both wave modes have dispersion, which is seen in Figure 1b. One of the modes is characterized by a lower critical frequency, but the frequency in this case is determined from equation (7) and is not equal to the critical frequency w_0 of the longitudinal wave. It can also be concluded that the dimensionless velocity parameters C_3 and C_4 used in solution (5) are asymptotic velocities of transverse bulk wave modes at $\omega \to \infty$.

Special Cases: Rayleigh and Lamb Waves

As a particular case, expressions (5) describe well-investigated solutions for the surface Rayleigh wave in the elastic half-space. Because the amplitude of displacement components of Rayleigh wave decays with depth (along the z axis), the constants for the exponent terms with positive indices in the expressions in solution (5) must be zero: $D_4 = D_5 = D_6 = 0$ and $E_4 = E_5 = E_6 = 0$. The boundary conditions at the surface $z = 0$ require normal forces and moments to be zero

$$\sigma_{zx}|_{z=0} = 0, \quad \sigma_{zy}|_{z=0} = 0, \quad \sigma_{zz}|_{z=0} = 0, \quad \mu_{zx}|_{z=0} = 0, \quad \mu_{zy}|_{z=0} = 0, \quad \mu_{zz}|_{z=0} = 0. \tag{8}$$

The substitution of solution (5) into the boundary conditions (8) at fixed k and ω, yields two independent solutions describing two different waves:

1. A Rayleigh wave with components u_x, u_z, and θ_y is determined by the dispersion equation $\det(\mathcal{M}_r(\nu_1, \nu_2, \nu_3)) = 0$, where (Kulesh *et al.*, 2005)

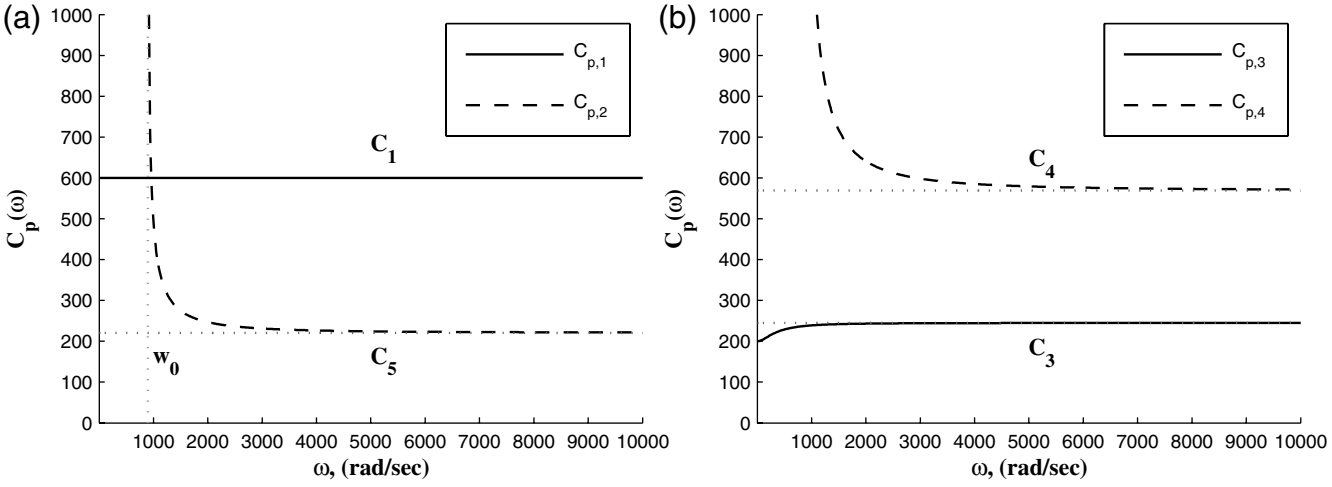

Figure 1. Numerical example illustrating the behavior of (a) longitudinal and (b) transverse bulk waves in the Cosserat continuum.

$$\mathcal{M}_r(p_1,p_2,p_3) = \begin{bmatrix} 2k^2-\frac{\omega^2}{C_2^2} & -2ikp_2 & -2ikp_3 \\ 2ikp_1 & 2k^2-\frac{\omega^2}{C_2^2} & 2k^2-\frac{\omega^2}{C_2^2} \\ 0 & p_2(A_m-\frac{\omega^2}{C_3^2}) & p_3(A_p-\frac{\omega^2}{C_3^2}) \end{bmatrix}.$$

2. A surface transverse wave with components u_y, θ_x, and θ_z has the following dispersion equation: $\det(\mathcal{M}_t(\xi_1,\xi_2,\xi_3)) = 0$, where (Kulesh *et al.*, 2006)

$$\mathcal{M}_t(p_1,p_2,p_3) = \begin{bmatrix} \frac{2ik}{1-B} & p_2(2+\frac{A_mC_4^2-\omega^2}{2A^2C_4^2}) & p_3(2+\frac{A_pC_4^2-\omega^2}{2A^2C_4^2}) \\ ikp_1(1+C) & p_2^2+k^2C & p_3^2+k^2C \\ (\frac{C_5^2}{C_4^2}-C-1)k^2-p_1^2\frac{C_5^2}{C_4^2} & ikp_2(1+C) & ikp_3(1+C) \end{bmatrix}.$$

metric media (solid lines). The dashed lines correspond to C_2 velocity. Thus, in the half-space whose dynamic behavior is described by the Cosserat model, in addition to the elliptic surface Rayleigh wave, it is also possible to observe another wave type, a surface wave whose one component is parallel to the boundary surface and perpendicular to the propagation direction. This wave mode does not have analogues in the classical elasticity theory. Both Rayleigh and surface transverse waves have the dispersive character of propagation in the half-space that also differs from the classical case.

Figures 2 and 3 show wavenumbers $k(\omega)$ and normalized phase velocities $C_p(\omega)/C_2$ for Rayleigh and surface transverse waves in the classical (dotted lines) and asym-

To investigate how a wave propagates in a free loaded plate with the thickness $2H$, let us consider the characteristic length $X_0 = H$. The boundary conditions in the dimension-

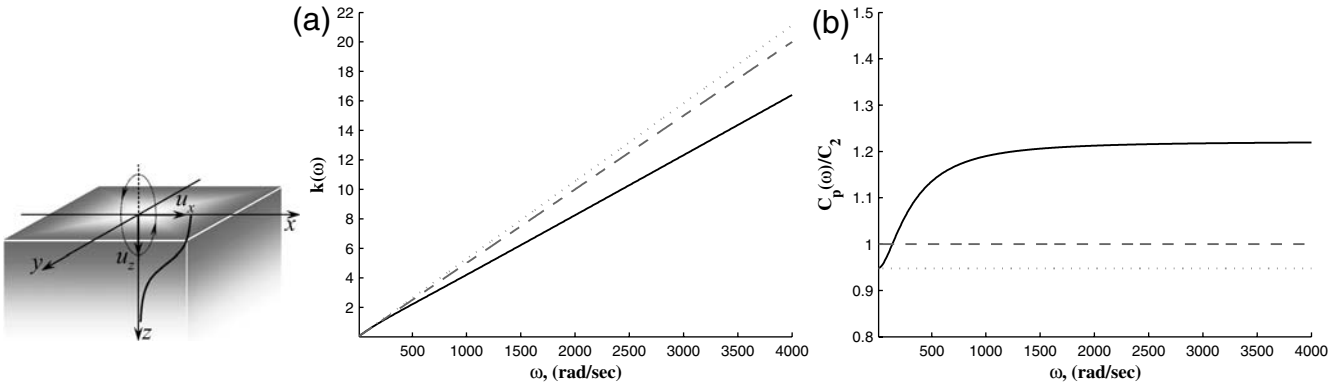

Figure 2. Numerical example illustrating the behavior of (a) wavenumber and (b) phase velocity for a Rayleigh wave in the Cosserat continuum.

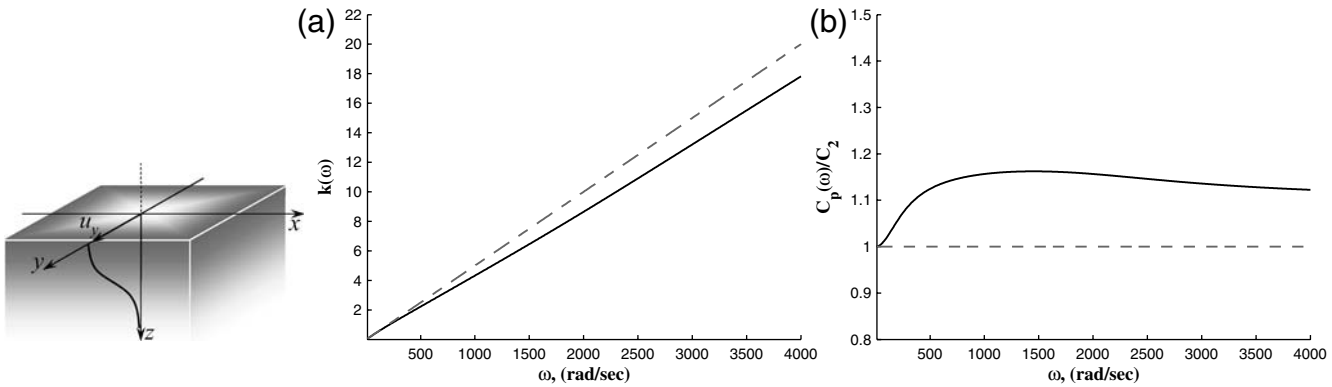

Figure 3. Numerical example illustrating the behavior of (a) wavenumber and (b) phase velocity for a surface transverse wave in the Cosserat continuum.

less form at the surfaces $z = \pm 1$ require the normal forces and moments to be zero:

$$\begin{aligned} &\sigma_{zx}|_{z=\pm 1} = 0, \quad \sigma_{zy}|_{z=\pm 1} = 0, \quad \sigma_{zz}|_{z=\pm 1} = 0, \\ &\mu_{zx}|_{z=\pm 1} = 0, \quad \mu_{zy}|_{z=\pm 1} = 0, \quad \mu_{zz}|_{z=\pm 1} = 0. \end{aligned} \tag{9}$$

The substitution of solution (5) into the boundary conditions (9) at fixed k and ω gives us two independent solutions for two wave types:

1. A Lamb wave with components u_x, u_z, and θ_y is described by the dispersion equation (Kulesh *et al.*, 2007)

$$\det\begin{bmatrix} \mathcal{M}_r(\nu_1,\nu_2,\nu_3)\cdot \mathrm{diag}(e^{-\nu_n}) & \mathcal{M}_r(-\nu_1,-\nu_2,-\nu_3)\cdot \mathrm{diag}(e^{\nu_n}) \\ \mathcal{M}_r(\nu_1,\nu_2,\nu_3)\cdot \mathrm{diag}(e^{\nu_n}) & \mathcal{M}_r(-\nu_1,-\nu_2,-\nu_3)\cdot \mathrm{diag}(e^{-\nu_n}) \end{bmatrix} = 0.$$

2. A transverse wave with components u_y, θ_x, and θ_z has the following dispersion equation (Kulesh *et al.*, 2007):

$$\det\begin{bmatrix} \mathcal{M}_t(\xi_1,\xi_2,\xi_3)\cdot \mathrm{diag}(e^{-\xi_n}) & \mathcal{M}_t(-\xi_1,-\xi_2,-\xi_3)\cdot \mathrm{diag}(e^{\xi_n}) \\ \mathcal{M}_t(\xi_1,\xi_2,\xi_3)\cdot \mathrm{diag}(e^{\xi_n}) & \mathcal{M}_t(-\xi_1,-\xi_2,-\xi_3)\cdot \mathrm{diag}(e^{-\xi_n}) \end{bmatrix} = 0.$$

In the previous expressions, $\mathrm{diag}(e^{-p_n}) \in \mathbb{C}^{3\times 3}$ is the diagonal matrix, and $(\cdot)$ is the scalar product.

Figure 4 shows wavenumbers $k(\omega)$ and normalized phase velocities $C_p(\omega)/C_2$ for the Lamb wave in the classical medium (dotted lines) and in the Cosserat medium (solid lines). The dashed lines correspond to C_1 and C_2 velocities of the classical medium. In Figure 5, the behavior is demonstrated for the new transverse wave in a layer. Thus, a qualitatively new wave mode with only one displacement component exists in a free loaded plate within the framework of the Cosserat medium besides well-investigated Lamb

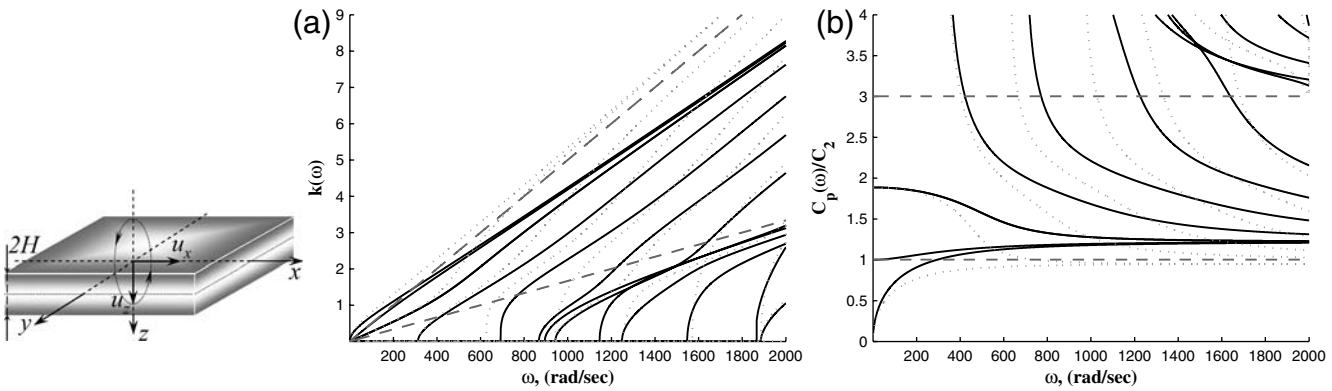

Figure 4. Numerical example illustrating the behavior of (a) wavenumber and (b) phase velocity for a Lamb wave in the Cosserat continuum.

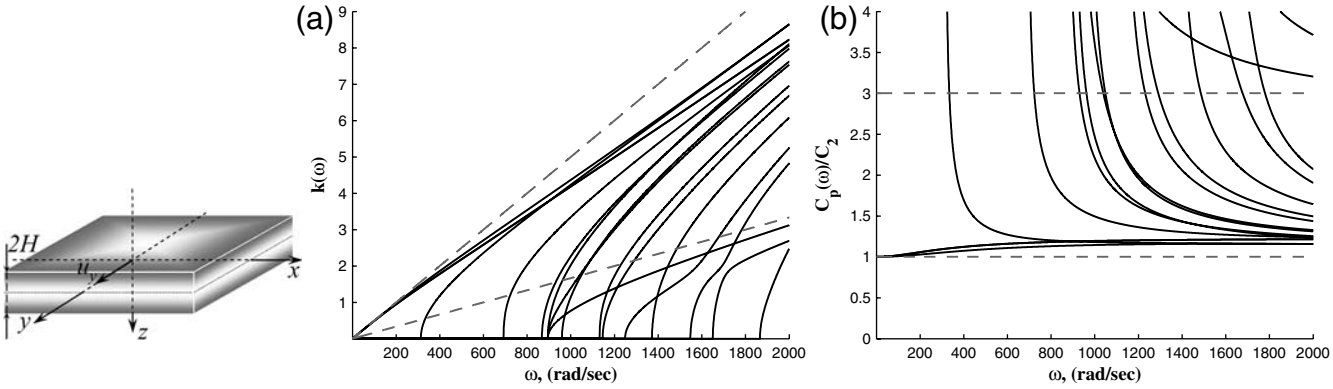

Figure 5. Numerical example illustrating the behavior of (a) wavenumber and (b) phase velocity for a transverse wave in the Cosserat continuum.

wave. As in the case of surface transverse wave, this new mode also does not have any analogy in the classical elasticity theory.

Conclusions

In this study, we discussed solutions for longitudinal and transverse bulk waves, Rayleigh wave, surface transverse wave in a half-space as well as Lamb wave and transverse wave in a thin layer within the framework of the isotropic Cosserat continuum.

Problems on bulk wave propagation (Fig. 1) are rather interesting from the viewpoint of interpretation of new parameters introduced for the dimensionless notation of wave solutions. However, these problems have no prospects from the standpoint of experimental implementation.

In contrast to bulk waves, surface waves for the elastic half-space have a considerable experimental potential. First, the dispersion analysis of experimental three-component seismograms allows construction of experimental dispersion curves and comparison with theoretical ones (Figs. 2 and 4). Second, rotation sensors make it possible to trace a relation between displacement and rotation components according to solution (5). Third, the presence of a transverse surface wave in the Cosserat continuum (Figs. 3 and 5) can also be the subject of experimental study with the use of sensors imbedded at different depths.

Data and Resources

Some plots were made using the Matlab Web site (http://www.mathworks.com/products/matlab/, last accessed June 2008).

Acknowledgments

This work was supported by the U.S. Civilian Research and Development Foundation (Post-Doctoral Fellowship Program Y2-P-09-04).

References

Aki, K., and P. G. Richards (2002). *Quantitative Seismology*, Second Ed., University Science Books, Sausalito, California.

Cosserat, E., and F. Cosserat (1909). *Theórie des Corps Déformables*, Hermann, Paris, France.

Eringen, A. C. (1998). *Microcontinuum Field Theories. I. Foundation and Solids*, Springer-Verlag, New York, New York.

Erofeev, V. I. (1999). *Wave Processes in Solids with Microstructure* (in Russian), Izd. Mosk. Gos. Univ., Moscow.

Gauthier, R. D, and W. E. Jahsman (1981). A quest for micropolar elastic constants. Part 2, *Arch. Mech.* **33,** no. 5, 717–737.

Igel, H., U. Schreiber, A. Flaws, B. Schuberth, A. Velikoseltsev, and A. Cochard (2005). Rotational motions induced by the M8.1 Tokachi-oki earthquake, September 25, 2003, *Geophys. Res. Lett.* **32,** L08309.

Kulesh, M. A., V. P. Matveenko, and I. N. Shardakov (2005). Construction and analysis of an analytical solution for the surface Rayleigh wave within the framework of the Cosserat continuum, *J. Appl. Mech. Tech. Phys.* **46,** no. 4, 556–563.

Kulesh, M. A., V. P. Matveenko, and I. N. Shardakov (2006). Propagation of surface elastic waves in the Cosserat medium, *Accoust. Phys.* **52,** no. 2, 186–193.

Kulesh, M. A., V. P. Matveenko, and I. N. Shardakov (2007). Constructing an analytical solution for Lamb waves using the Cosserat continuum approach, *J. Appl. Mech. Tech. Phys.* **48,** no. 1, 119–125.

Kulesh, M. A., V. P. Matveenko, M. V. Ulitin, and I. N. Shardakov (2008). Analysis of the wave solution of the elastokinetic equations of a Cosserat continuum for the case of bulk plane waves, *J. Appl. Mech. Tech. Phys.* **49,** no. 2, 323–329.

Lakes, R. S. (1995). Experimental methods for study of Cosserat elastic solids and other generalized continua, in *Continuum models for materials with micro-structure*, H. Muhlhaus (Editor), J. Wiley, New York, New York, 1–22.

Lyalin, A. E., V. A. Pirozhkov, and R. D. Stepanov (1982). On the propagation of surface waves in a Cosserat continuum, *Akust. Zh* **28,** no. 6, 838–840.

Nigbor, R. L. (1994). Six-degree-of-freedom ground-motion measurement, *Bull. Seismol. Soc. Am.* **84,** no. 5, 1665–1669.

Nowacki, W. (1975). *Theory of Elasticity* (in Russian), Mir, Moscow.

Savin, G. N., A. A. Lukashov, and E. M. Lysko (1970). Propagation of elastic waves in a Cosserat continuum with constrained rotation, *Prikl. Mekh.* **6,** no. 6, 37–41.

Twiss, R. J., B. J. Souter, and J. R. Unruh (1993). The effect of block rotations on the global seismic moment tensor and the patterns of seismic *P* and *T* axes, *J. Geophys. Res.* **98,** no. B1, 645–674.

Institute of Continuous Media Mechanics
Ural Division, Russian Academy of Sciences
Perm 614013, Russia
kma@icmm.ru

Manuscript received 25 June 2008